(Received 15 January 2026, Accepted 24 February 2026, Scheduled 26 March 2026)

Multi-Band Double-Sided Printed Dipole Antenna for Sub-6 GHz Bands of 5G Network

Tarit Sarkar[1,*], R. P. Ghosh[1], and R. R. Pal[2]

[1] *Department of Electronics, Vidyasagar University, Midnapore, West Bengal, India*
[2] *Department of Physics, Vidyasagar University, Midnapore, West Bengal, India*

ABSTRACT: The Fifth-Generation (5G) radio network consists of two spectrums: one millimeter-wave band (24–40 GHz) and the other below 6 GHz, which is also popularised as sub-6 GHz band. The spectrum of a sub-6 GHz radio network may be divided into three bands, i.e., low-band (below 1 GHz), mid-band (1–2.6 GHz), and upper mid-band (3.5–6 GHz). The low-band provides a good network coverage, and the mid-band offers a balance between coverage and capacity, whereas the high-band provides a super data capacity and speed. The service providers use combinations of different bands from these three segments of sub-6 GHz spectrum to deliver smooth 5G services. In this work, a novel design of a multiband Double Sided Printed Dipole Antenna (DSPDA) system is proposed that operates at least at one band in each segment of the sub-6 GHz spectrum. The design consists of two DSPDAs, a symmetric one and an asymmetric one, fed in series by a common line in a tree-like structure. The multiple bands are obtained by having fundamental resonant frequencies and their harmonics. All bands are predictable by the design equations. It also provides the flexibility of choosing any band of operation. The antenna is experimentally verified.

1. INTRODUCTION

The 5G radio network has revolutionized mobile communication, interconnectivity between devices such as Internet of Things (IoT) and applications such as smart vehicles, smart energy, and medical applications. It can efficiently transfer data due to ultra-low latency, large network capacity, andh igh data speed with high reliability; hence, users experience quality wireless connectivity [1–5]. The 5G spectrum may be divided into two highly distinct bands. One operating at above 24 GHz, known as the millimeter wave-band, and the other below 6 GHz, designated as sub-6 GHz band.

The millimeter-wave band ranges between 24 and 40 GHz and provides extremely high speed and data capacity, though the coverage area is small.

Sub-6 GHz bands are presently in use for mobile communication, also containing 2G, 3G, and 4G bands. The sub-6 GHz band may be divided into three segments. The low-band operates below 1 GHz; the mid-band ranges between 1 and 2.6 GHz; and the upper mid-band falls between 3.5 and 6 GHz. The major service providers use different combinations of these frequency bands for efficient data transfer. The sub-6 GHz band, which is widely spaced from below 1 GHz to nearly 5 GHz, is important for 5G radio links as it provides better coverage and penetration through obstacles, such as walls and buildings, and supports the high-speed data communication for Internet of Things (IoT) devices, etc.

The lower-band consists of n28(700 MHz), n20(800 MHz), n5(850 MHz), n8(900 MHz) frequencies. The low-band has decent network coverage with a smaller bandwidth. These bands are suitable for rural and indoor environments. These frequency bands are used in Smart farming, soil moisture sensors, crop health monitoring via IoT, remote patient monitoring in rural areas, emergency communication, disaster alerts, basic IoT sensors, GPS trackers, smart meters, etc.

The mid- and upper-mid bands offer good stability between coverage and capacity. The mid-band has the sub-bands of n3(1800 MHz), n2(1900 MHz), n1(2100 MHz), n40(2300 MHz), n41(2500 MHz). The upper mid-band consists of n78(3500 MHz), n77(3700 MHz), n79(4900 MHz) bands. The mid-bands and upper-bands are widely used in urban and suburban environments due to their high speed and coverage. It has widespread applications like traffic management, smart lighting, surveillance, virtual classrooms, remote learning, video conferencing, connected vehicles, traffic lights coordination, mobile telemedicine, e-health services, etc.

The mm-wave band and sub-6 GHz band are widely separated. Hence, it is a difficult task to cover these two bands using a single-element antenna. Till now, no work has been reported covering both these bands using a single antenna. Two separate antennas are required to operate in the two bands. Though a multiport antenna system is reported to cover all these bands [6], it consists of a four-element array to operate in the mm-band (28 GHz) and offers a reconfigurable radiation pattern. Also, to cover the sub-6 GHz bands, two antennas have been used. The whole antenna system covers all the 5G bands. Other than this work, several works have been reported in the range of sub-6 GHz [7–12].

Kumar et al. propose a 1×2 defected ground structure (DGS)-based fractal multiple-input multiple-output (MIMO) antenna array, covering frequencies in the sub-6 GHz bands,

* Corresponding author: Tarit Sarkar (taritsarkar8@gmail.com).

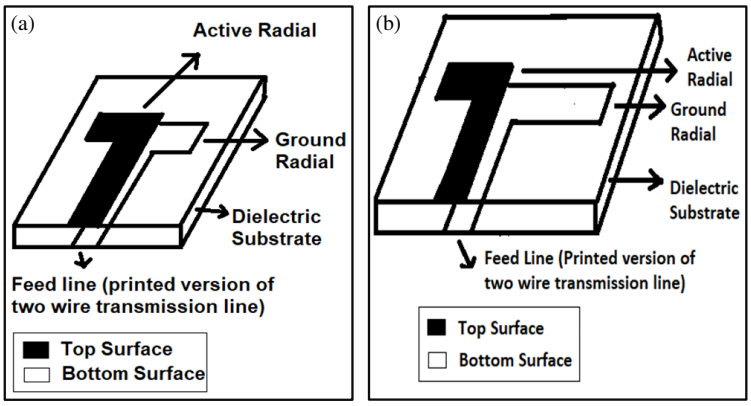

FIGURE 1. Geometry of (a) symmetric DSPDA, (b) asymmetric DSPDA [25].

such as 0.7 GHz, 2.6 GHz, 3.1 GHz, and 3.5 GHz [7]. Another antenna with a DGS is reported by Dhananjeyan et al. to improve both bandwidth and port-to-port isolation in the range of 3.2–3.8 GHz [8]. Ciydem and Miran report a suspended patch antenna that covers the n78 band (3.3–3.8 GHz). The antenna consists of a parasitic patch, two modified L-probe feeds, and a vertical metal wall [9]. A novel dual-polarized antenna is proposed by Alieldin et al. for the n78 band [10]. Xue et al. develop a compact dual-polarized antenna, which has a wide impedance bandwidth of 25.6% and a low cross-polarization ratio of about 22 dB, although it covers only the n78 band [11]. Another patch antenna is reported by Liu et al., designed by integrating a dual-mode coupled patch, four planar coupled strips, and four shorted strips around it, which covers the n78 (3.3–3.8 GHz) and n79 (4.8–5.0 GHz) bands [12].

Ta et al. develop a broadband printed-dipole antenna and its arrays for 5G wireless cellular networks in 26.5–38.2 GHz [13]. Fan et al. propose an array of printed dipole antennas, which has the impedance bandwidth of 50% (24–40 GHz) and beam scanning ability [14]. Karthikeya et al. report an electrically compact end-fire antenna with a high gain of about 10 dBi operating in the 28 GHz [15].

Several broadband antennas have been reported covering the mm-band of 5G spectrum [16–18]. A magneto-electric dipole antenna with a claw-shaped reflector is reported for 5G communication systems. Here, a pair of E-shaped radiating patches is used to form an electric dipole, and two folded patches shorted to the ground are used as the magnetic dipole. It provides a wide relative bandwidth of 103.6% with the center frequency of 2.45 GHz [16]. Another magneto-electric dipole with circular polarization is reported by Sun et al. for a 5G Wi-Fi application operating in 4.98–6.31 GHz [17]. Feng et al. report a wideband antenna using a metasurface for 5G communications. It provides a wide impedance bandwidth of 77.2% in 1.63–3.68 GHz [18].

Multiband antennas have been reported by several researchers [19–22]. A slotted conical patch is incorporated in a triangular patch, connected by a single feed line, and it provides multiple bands at 2.450–2.495 GHz, 5.0–6.3 GHz, and 23–28 GHz [19]. Zhou et al. report an antenna system consisting of two square loop antennas with two parasitic loops to perform at multiple frequency bands, i.e., 1.71–2.69 GHz, 3.3–3.6 GHz, and 4.8–5 GHz [20]. Elechi and John propose a multiband rectangular patch antenna at 3.5 GHz, 5.93 GHz, 7.49 GHz, 10.07 GHz, and 11.65 GHz, but most of the bands are not used for 5G applications [21]. He et al. report an antenna system consisting of three different arrays, i.e., an aperture antenna array, a 2×2 antenna array, and a 4×4 antenna array is designed to operate in three different frequency bands at 0.69–0.96 GHz, 1.8–2.7 GHz, and 3.3–3.8 GHz, respectively [22], but the whole antenna system is complicated in design and does not follow any specific design rule. The antennas reported so far operate in a portion of the sub-6 GHz spectrum, covering either low, middle, or high frequency bands.

Even 5G antennas used in terminals of Fixed Wireless Access (FWA), Industrial & Commercial LTE/5G deployments, Oil & Gas communication systems, and Power, Energy & Water telemetry access, etc., are complex in structure and are not completely two-dimensional [23, 24]. The dimensions of these antennas are larger than our two-antenna system. The minimum dimension of an antenna is found with the length of 146 mm, width of 134 mm, and height of 26 mm [24], whereas, our reported antenna has the length, width, and height of 125 mm, 70 mm, and 1.6 mm. A comparative study is tabulated in Table 1.

In our work, a multiband printed dipole two-antenna system with a simple design is proposed, which operates in the low, mid, and upper mid-bands of the sub-6 GHz spectrum. The multiband characteristics of the printed dipole antenna are achieved by using two DSPDAs: an asymmetric DSPDA and a symmetric DSPDA with a common feed structure. Moreover, operating bands are tunable with the change of the length of the arms.

In a DSPDA, the two arms are printed on the opposite surfaces of a dielectric substrate. It may be symmetric in terms of its length, width, etc., as shown in Figure 1(a) [25]. The symmetric DSPDA resonates at a single frequency, whereas the asymmetric DSPDA has two arms which are not similar in length, as shown in Figure 1(b) [25]. These two arms resonate at two different frequencies. The multiband feature is achieved by using their fundamental frequencies and by excit-

TABLE 1. Comparative study of related work.

Ref. & year	DK & tan δ of the substrate	Types of antenna	Oprating bands (in GHz)	Size of the antenna	Gain (dBi)
[7] 2024	DK $= 4.4$ & $\tan\delta = 0.02$	DGS-based fractal MIMO antenna array	**4** (0.7, 2.6, 3.1, & 3.5 GHz)	$195 \times 52 \times 1.6\,\text{mm}^3$	Min gain $= 7.9$, Max gain $= 12.9$
[12] 2024	DK $= 3.55$ & $\tan\delta = 0.002$	Coupled resonator and shorted strips	**2** (3.24–3.83 GHz and 4.74–5.30 GHz)	$0.34\lambda_L \times 0.34\lambda_L \times 0.11\lambda_L$ Corresponding $\lambda_L = 3.24$ GHz	Avg. gain $= 8.4$
[19] 2020	DK $= 2.2$ & $\tan\delta = 0.0009$	Slotted conical patch antenna	**2** (2.45–2.49 & 5–6.3 GHz)	$[0.35\lambda_0 * 0.35\lambda_0 * 0.004\lambda_0]$ Corresponding $f_0 = 2.4$ GHz	Avg gain = around 3.55–4.7
[20] 2021	DK $= 3.66$ & $\tan\delta = 0.02$	Aperature antenna using FSS (not completely planar)	**3** (1.60–2.70, 3.28–3.80, & 4.75–5.18 GHz)	$140 \times 55 \times 0.76\,\text{mm}^3$	Avg. gain = around 9.1
[22] 2021	DK $= 4.4$ & $\tan\delta = 0.02$	Aperature antenna array (not completely planar)	**3** (0.69–0.96, 1.8–2.7, & 3.3–3.8 GHz)	$0.69\lambda_L \times 0.69\lambda_L \times 0.177\lambda_L$ Corresponding $\lambda_L = 0.69$ GHz	Min. gain $= 6.5$, Max gain $= 8.2$
Our work	DK $= 3$ & $\tan\delta = 0.025$	Completely planar printed dipole antenna	**5** (0.85–1.46, 1.83–2.24, 2.28–2.41, 3.02–4.61, & 4.75–5.84 GHz)	$[0.379\lambda_0 * 0.21\lambda_0 * 0.004\lambda_0]$ Corresponding $f_0 = 0.90$ GHz	Min. gain $= 3$, Max gain $= 5.80$

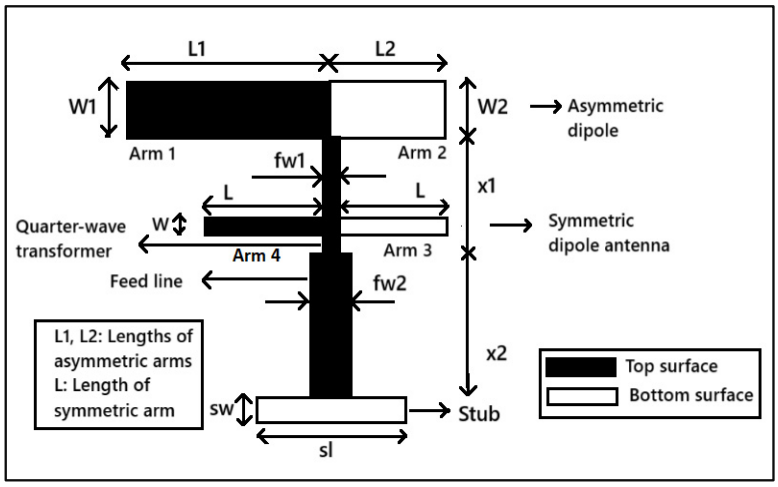

FIGURE 2. The structure of the multiband antenna.

ing their first harmonics. The symmetric DSPDA has one fundamental frequency and its harmonics, whereas the asymmetric DSPDA has two fundamental frequencies and its harmonics. The antennas have been designed in such a way that they provide the desired multiband feature used in the sub-6 GHz bands. A quarter-wave transformer and a stub are used for better impedance matching. The feed line of the antenna system is a printed version of the two parallel wire transmission lines [26].

The design equations to predict the resonant frequencies for the symmetric DSPDA and asymmetric DSPDA are reported by Ghosh et al. [27] and Sarkar et al. [28], and are given in Equations (1) and (2), respectively. The resonant frequency depends on the length of the arms only, and it does not depend upon the antenna width for $w/h \geq 3.94$, as reported by the authors.

$$f_r = \frac{C}{4\sqrt{\epsilon_r}} * \frac{1}{L_0} * \frac{1}{0.6463 * e^{-0.4792\epsilon_r} + 0.5453 * e^{-0.01283\epsilon_r}} \quad (1)$$

$$f_r = \frac{C}{4\sqrt{\epsilon_r}} * \frac{1}{L_0} * \frac{1}{0.8528 * e^{-0.1295\epsilon_r} + 0.0001885 * e^{1.179\epsilon_r}} \quad (2)$$

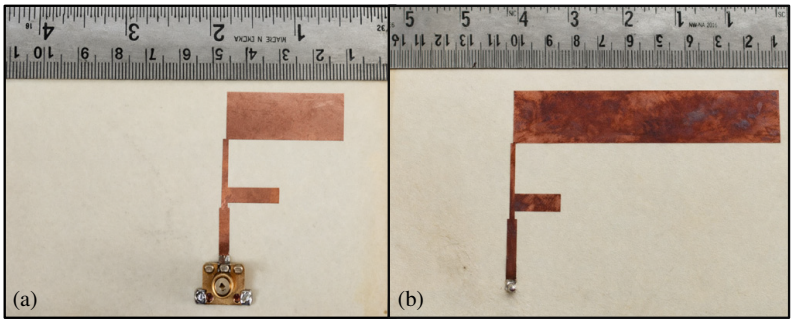

FIGURE 3. The images of the fabricated antenna, (a) active radial, (b) ground radial.

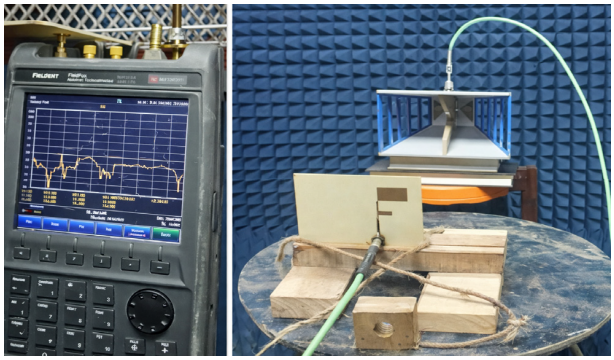

FIGURE 4. The measurement setup for the S_{11}, and the radiation patterns.

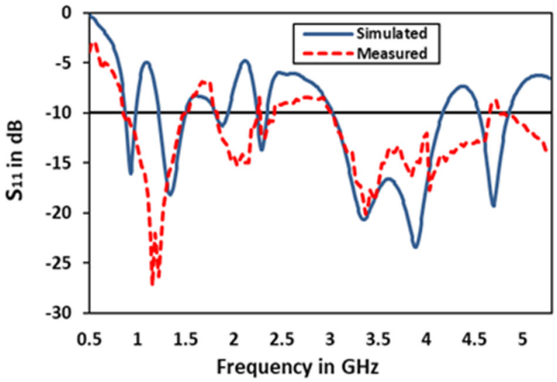

FIGURE 5. The simulated and measured S_{11} plots of the antenna.

TABLE 2. Frequency bands covered by the antenna system.

Name of Antennas	Lengths of arms	Resonating/Fundamental frequencies	First harmonics	Covered bands of 5G spectrum
Asymmetric DSPDA	L1 (Arm-1)	900 MHz	1800 MHz	n8 and n2
	L2 (Arm-2)	2300 MHz	4600 MHz	n40 and n79
Symmetric DSPDA	L (Arm-3 & Arm-4)	3700 MHz	7400 MHz	n77

where C is the speed of light in free space, f_r the resonant frequency, ϵ_r the Dielectric Constant (DK) of the material, and L_0 the length of one arm.

2. ANTENNA DESIGN

A multiband two-antenna system to operate in the sub-6 GHz bands is designed using two DSPDAs connected in series through a common feed line. The antenna structure is shown in Figure 2. The antenna system takes the form of a tree, having the feed line as the trunk and antenna arms as its branches. However, it does not form either an antenna array or a Log Periodic Dipole Array (LPDA).

The asymmetric DSPDA is placed on top of the structure. The asymmetric DSPDA has two arms with different lengths, Arm-1 & Arm-2. They are designed to resonate at 900 MHz and 2300 MHz. The width of the antennas has been widened for better impedance bandwidth. Beneath it, there is a quarter-wave transformer.

TABLE 3. Dimensions of the antenna system.

Name of antenna	Lengths of arms		Width of arms	
Asymmetric DSPDA	L1 (Arm-1)	L2 (Arm-2)	W1 (Arm-1)	W2 (Arm-2)
	84.54 mm	35 mm	16 mm	16 mm
Symmetric DSPDA	L=18 mm		W=5 mm	
Feed Network				
	Length		**Width**	
Quarter-wave transformer	x1=22 mm		fw1=1.5 mm	
Feed line	x2=28 mm		fw2=3 mm	
Stub	sl=16 mm		sw=4.5 mm	

The symmetric DSPDA is placed just below the quarter-wave transformer. The arms (Arm-3 & Arm-4) are equal in

TABLE 4. Bands covered by the antenna.

Available frequency bands for 5G New Radio			Simulated bands (MHz)	Measured bands (MHz)	Gain & Efficiency
Band name	Uplink (MHz)	Downlink (MHz)			
n8	880–915	925–960	860–990	850–1462	2.2 dBi & ∼97%
n2	1850–1910	1930–1990	1780–1960	1839–2242	3.5 dBi & ∼99%
n40	2300-2400		2230–2360	2280–2410	4.5 dBi & ∼99%
n77	3300–4200		3030–4200	3028–4614	5.79 dBi & ∼99%
n79	4400–5000		4540–4880	4750–5840	3.5 dBi & ∼98%

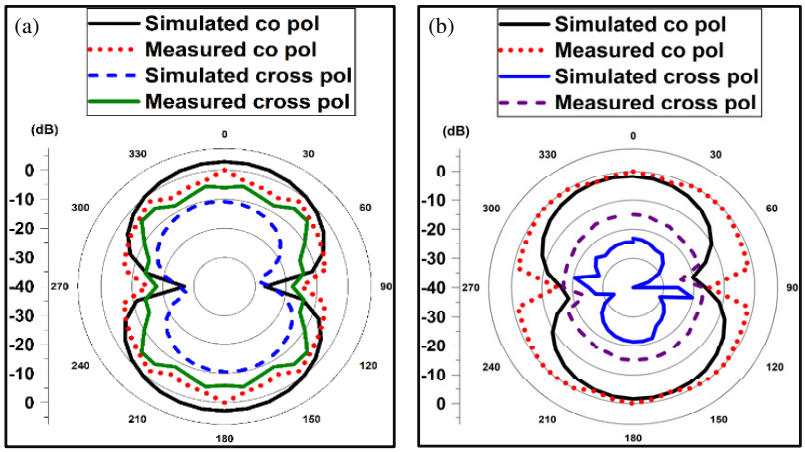

FIGURE 6. Normalised radiation patterns at 0.90 GHz, (a) E-plane, (b) H-plane.

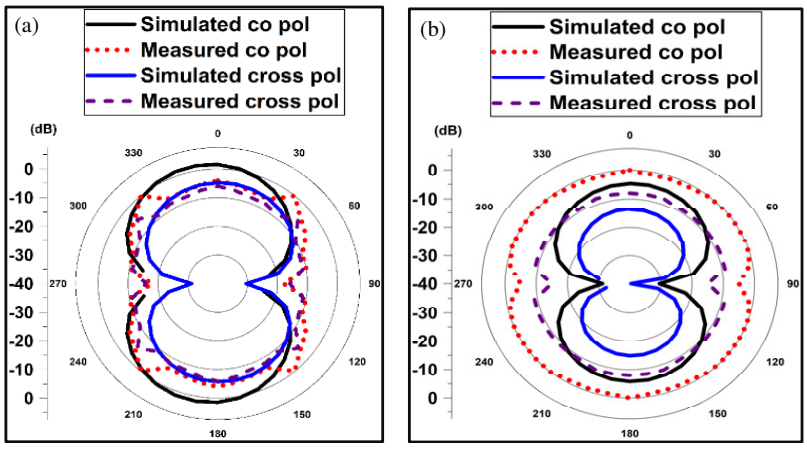

FIGURE 7. Normalised radiation patterns at 1.80 GHz, (a) E-plane, (b) H-plane.

length and hence resonate at one frequency only. The length has been designed so that DSPDA resonates at 3700 MHz. A stub is connected at the bottom of the feed line for better impedance matching.

The proposed antenna has three fundamental frequencies, and its harmonics are excited to get the multiband characteristic. The fundamental frequency (3700 MHz) and the first harmonic of 2300 MHz are stagger-tuned to get the entire upper-mid band. The scattering problem related to the interaction of the antenna radiation with other hardware of the end terminal may be analysed by semi-analytical modelling like the use of auxiliary sources [29–30]. The covered frequency bands with corresponding arms are tabulated in Table 2.

The antennas are designed on the material with the following specifications.

Dielectric constant (DK) = 3, Height of the substrate $(h) = 1.54$ mm, Loss tangent $(\tan\delta) = 0.0025$.

The arm lengths are calculated using Equations (1) and (2). The dimensions of the antenna system are tabulated in Table 3.

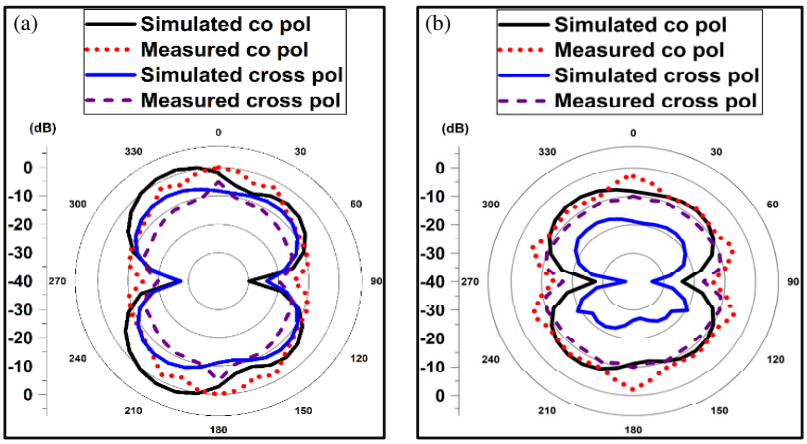

FIGURE 8. Normalised radiation patterns at 2.30 GHz, (a) E-plane, (b) H-plane.

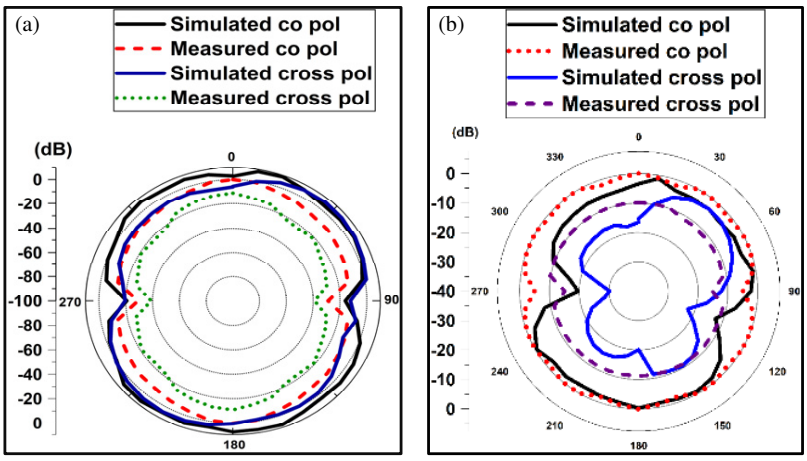

FIGURE 9. Normalised radiation patterns at 3.70 GHz, (a) E-plane, (b) H-plane.

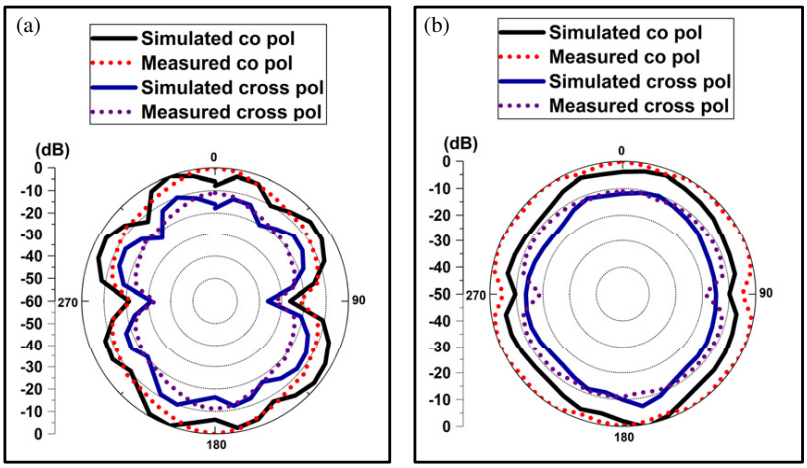

FIGURE 10. Normalised radiation patterns at 4.80 GHz, (a) E-plane, (b) H-plane.

3. RESULTS AND DISCUSSIONS

The proposed antenna has been simulated in the Finite Element Method (FEM)-based Computer Simulation Technology (CST) Microwave Studio [31]. It is fabricated for experimental verification. The images of the fabricated antenna are shown in Figure 3.

The experimental setup for characterisation of the antenna is shown in Figure 4. The simulated and measured S_{11} of the antenna are shown in Figure 5. The experimental result closely

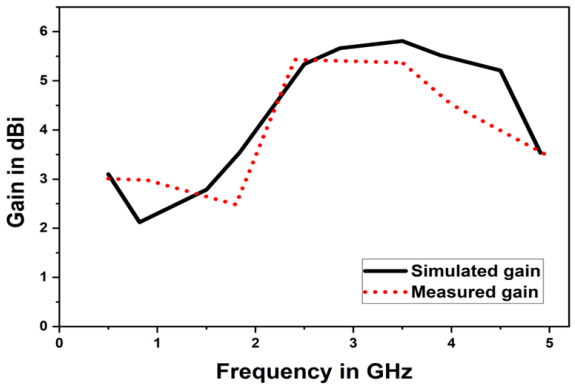

FIGURE 11. The gain vs. frequency plots.

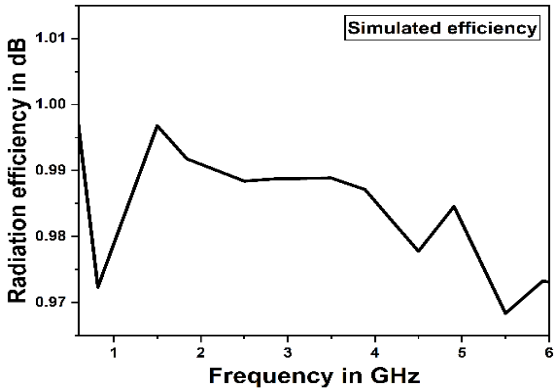

FIGURE 12. The simulated efficiency vs. frequency plot.

matches the simulated one. A comparison table of available bands in sub-6 GHz and the bands covered by the antenna is shown in Table 4. The antenna is linearly polarised. The cross-polar discrimination is within the acceptable limit.

The normalized E-plane and H-plane radiation patterns of the antenna at the frequencies of 0.90 GHz, 1.80 GHz, 2.30 GHz, 3.70 GHz, and 4.80 GHz are shown in Figures 6, 7, 8, 9, and 10, respectively. The E and H plane radiation patterns are stable throughout the bands. The cross-polar discrimination is within the acceptable limit, i.e., 10–12 dB. The dipole antenna provides omnidirectional characteristics in the H-plane; hence, it may provide a good coverage in indoor environments. The gain vs. frequency plot of the antenna is shown in Figure 11. The antenna has the minimum gain of about 3 dBi and the maximum gain of about 5.80 dBi. The proposed antenna provides about 98% radiation efficiency, as shown in Figure 12.

4. CONCLUSIONS

A simple and novel design of a multiband two-antenna system is proposed to operate in five radio bands (n2, n8, n40, n77, and n79) of the sub-6 GHz bands of the 5G radio network. The multiband antennas operating in sub-6 GHz bands reported so far are either complex in structure or working in an array environment. The antenna structure uses a symmetrical DSPDA and an asymmetrical DSPDA. The resonant frequencies are predictable by closed-form expressions reported by the authors. The design equation provides flexibility to design an antenna in any combination of operating bands. It is also mentioned that no multiband antenna is reported yet whose resonant frequencies are predictable by a design equation considering the large number of bands it is covering. Though two antennas have been used, they do not work in either an array environment or LPDA. The size of the antenna system has not been increased appreciably either.

ACKNOWLEDGEMENT

The authors express gratitude to the DST & Biotec., Govt. of West Bengal, India, for their financial support.

REFERENCES

[1] Xiang, W., K. Zheng, and X. Shen, *5G Mobile Communications*, Springer, 2016.

[2] Ahmed, A. M., S. A. Hasan, and S. A. Majeed, "5G mobile systems, challenges and technologies: A survey," *Journal of Theoretical and Applied Information Technology*, Vol. 97, No. 11, 3214–3226, 2019.

[3] Biradar, S. B. and G. G. Hallur, "Economic implication of spectrum bands used in 5G: A multicountry study of spectrum allocation," in *2022 International Conference on Decision Aid Sciences and Applications (DASA)*, 584–590, Chiangrai, Thailand, Mar. 2022.

[4] Liu, D., W. Hong, T. S. Rappaport, C. Luxey, and W. Hong, "What will 5G antennas and propagation be?" *IEEE Transactions on Antennas and Propagation*, Vol. 65, No. 12, 6205–6212, Dec. 2017.

[5] Suganya, E., T. A. J. M. Pushpa, and T. Prabhu, "Advancements in patch antenna design for sub-6 GHz 5G smartphone application: A comprehensive review," *Wireless Personal Communications*, Vol. 137, No. 4, 2217–2252, Aug. 2024.

[6] Liang, Q., H. Aliakbari, and B. K. Lau, "Co-designed millimeter-wave and sub-6 GHz antenna for 5G smartphones," *IEEE Antennas and Wireless Propagation Letters*, Vol. 21, No. 10, 1995–1999, Oct. 2022.

[7] Kumar, A., G. Singh, M. K. Abdulhameed, S. R. Hashim, and A. J. A. Al-Gburi, "Development of fractal 5G MIMO antenna for sub 6 GHz wireless automotive applications," *Progress In Electromagnetics Research M*, Vol. 130, 121–128, 2024.

[8] Dhananjeyan, R., M. Pant, K. Vishalatchi, S. Janarthanan, P. Sukumar, D. S. S. Raja, and D. Rajeshkumar, "High-performance compact antenna for sub-6 GHz 5G MIMO applications," *Progress In Electromagnetics Research C*, Vol. 157, 57–63, 2025.

[9] Ciydem, M. and E. A. Miran, "Dual-polarization wideband sub-6 GHz suspended patch antenna for 5G base station," *IEEE Antennas and Wireless Propagation Letters*, Vol. 19, No. 7, 1142–1146, Jul. 2020.

[10] Alieldin, A., Y. Huang, M. Stanley, S. D. Joseph, and D. Lei, "A 5G MIMO antenna for broadcast and traffic communication topologies based on pseudo inverse synthesis," *IEEE Access*, Vol. 6, 65 935–65 944, 2018.

[11] Xue, K., D. Yang, C. Guo, H. Zhai, H. Li, and Y. Zeng, "A dual-polarized filtering base-station antenna with compact size for 5G applications," *IEEE Antennas and Wireless Propagation Letters*, Vol. 19, No. 8, 1316–1320, Aug. 2020.

[12] Liu, X., B. Sanz-Izquierdo, H. Zhang, S. Gao, W. Hu, X.-X. Yang, and J. T. S. Sumantyo, "Differentially fed dual-band base station antenna with multimode resonance and high selectivity for 5G applications," *IEEE Transactions on Antennas and Propagation*, Vol. 72, No. 1, 256–266, 2024.

[13] Ta, S. X., H. Choo, and I. Park, "Broadband printed-dipole antenna and its arrays for 5G applications," *IEEE Antennas and Wireless Propagation Letters*, Vol. 16, 2183–2186, May 2017.

[14] Fan, F.-F., Q.-L. Chen, Y.-X. Xu, X.-F. Zhao, J.-C. Feng, and Z.-H. Yan, "A wideband compact printed dipole antenna array with SICL feeding network for 5G application," *IEEE Antennas and Wireless Propagation Letters*, Vol. 22, No. 2, 283–287, Feb. 2023.

[15] Karthikeya, G. S., S. K. Koul, A. K. Poddar, and U. Rohde, "Ultra-compact orthogonal pattern diversity antenna module for 5G smartphones," *Microwave and Optical Technology Letters*, Vol. 63, No. 8, 2003–2012, 2021.

[16] Zhang, X., Y.-C. Jiao, Z.-B. Weng, Y.-X. Zhang, and S. Feng, "Wideband magneto-electric dipole antenna with a claw shaped reflector for 5G communication systems," *Microwave and Optical Technology Letters*, Vol. 61, No. 9, 2098–2104, 2019.

[17] Sun, K., D. Yang, and S. Liu, "A wideband hybrid feeding circularly polarized magneto-electric dipole antenna for 5G Wi-Fi," *Microwave and Optical Technology Letters*, Vol. 60, No. 8, 1837–1842, 2018.

[18] Feng, B., L. Li, Q. Zeng, and K. L. Chung, "A wideband antenna using metasurface for the 2G/3G/LTE/5G communications," *Microwave and Optical Technology Letters*, Vol. 60, No. 10, 2482–2487, 2018.

[19] Khan, Z., M. H. Memon, S. U. Rahman, M. Sajjad, F. Lin, and L. Sun, "A single-fed multiband antenna for WLAN and 5G applications," *Sensors*, Vol. 20, No. 21, 6332, 2020.

[20] Zhou, G.-N., B.-H. Sun, Q.-Y. Liang, S.-T. Wu, Y.-H. Yang, and Y.-M. Cai, "Triband dual-polarized shared-aperture antenna for 2G/3G/4G/5G base station applications," *IEEE Transactions on Antennas and Propagation*, Vol. 69, No. 1, 97–108, Jan. 2021.

[21] Elechi, P. and P. O. R. John, "Improved multiband rectangular microstrip patch antenna for 5G application," *Journal of Telecommunication, Electronic and Computer Engineering (JTEC)*, Vol. 14, No. 2, 7–14, 2022.

[22] He, D., Y. Chen, and S. Yang, "A low-profile triple-band shared-aperture antenna array for 5G base station applications," *IEEE Transactions on Antennas and Propagation*, Vol. 70, No. 4, 2732–2739, 2022.

[23] https://www.poynting.tech.

[24] https://www.taoglas.com.

[25] Garg, R., P. Bhartia, I. Bahl, and A. Ittipiboon, *Microstrip Antenna Design Handbook*, 399–402, Artech House, 2001.

[26] Wheeler, H. A., "Transmission-line properties of parallel strips separated by a dielectric sheet," *IEEE Transactions on Microwave Theory and Techniques*, Vol. 13, No. 2, 172–185, 1965.

[27] Ghosh, R. P., K. Patra, B. Gupta, and S. K. Chowdhury, "Accurate formula to determine resonant frequency of double sided printed dipole antenna," *IETE Journal of Research*, Vol. 64, No. 3, 331–336, 2018.

[28] Sarkar, T., R. P. Ghosh, and R. R. Pal, "Closed form expression to predict the resonant frequencies of a dual band asymmetric double-sided printed dipole antenna," *International Journal of Electronics*, Vol. 113, No. 1, 24–38, 2026.

[29] Valagiannopoulos, C. A., N. L. Tsitsas, and G. Fikioris, "Convergence analysis and oscillations in the method of fictitious sources applied to dielectric scattering problems," *Journal of the Optical Society of America A*, Vol. 29, No. 1, 1–10, 2012.

[30] Kakulia, D., K. Tavzarashvili, G. Ghvedashvili, D. Karkashadze, and C. Hafner, "The method of auxiliary sources approach to modeling of electromagnetic field scattering on two-dimensional periodic structures," *Journal of Computational and Theoretical Nanoscience*, Vol. 8, No. 8, 1609–1618, 2011.

[31] CST Corporation, "CST Microwave Studio," [Online]. Available: http://www.cst.com, 2022.